2012 IEEE International Conference on Robotics and Automation
RiverCentre, Saint Paul, Minnesota, USA
May 14-18, 2012

Design and development of a soft robot with crawling and grasping capabilities

Marcello Calisti, *Student Member, IEEE*, Andrea Arienti, Federico Renda, Guy Levy, Binyamin Hochner, Barbara Mazzolai, *Member, IEEE*, Paolo Dario, *Fellow Member, IEEE*, and Cecilia Laschi, *Member, IEEE*

***Abstract*— This paper describes the design and development of a robot with six soft limbs, with the dual capability of pushing–based locomotion and grasping by wrapping around objects. Specifically, a central platform lodges six silicone limbs, radially distributed, with cables embedded. A new mechanism–specific gait, invariant regarding the number of limbs, has been implemented. Functionally, some limbs provide stability while others push and pull the robot to locomote in the desired direction. Once the robot is close to a target, one limb is elected to wrap around the object and, thanks to the particular limb structure and the soft material, a friction–based grasping is achieved. The robot is inspired by the octopus and implements the key principles of locomotion in this animal, without coping the full body structure. For this reason it works in water, but it is not restricted to this environment. The experiments show the effectiveness of the original solution in locomotion and grasping.**

I. INTRODUCTION

Traditional robots, composed by stiff links and joints, are built of hard materials. They have high accuracy, they can carry heavy loads and they are easy to control. They usually work in structured environments and their constitutive material can not be deformed. On the other hand there is a new kind of robots, so called soft robots, that are composed by soft materials. Their soft structure can be deformed, they have high compliance to obstacles and they are intrinsically safe. For this kind of robots, controllability, accuracy and effectiveness are challenging tasks [1].

Most of these soft robots are able to crawl on various surfaces, but cannot perform any other task. In some cases the locomotion is inspired by animals, as from the crawling of the earthworm [2] or from the peristaltic locomotion of the *Oligochaeta* [3],[4]. In other cases they are built from scratch: in [5] a robot is presented, made of shape memory alloys, which is able to jump and roll; in [6] a robot is presented that crawls changing stiffness and shape.

On the other hand, soft manipulators are developed, that use traditional solution to move. To our knowledge the OctArm is the most studied. This is composed by air muscle actuators roughly resembling the McKibben actuators. OctArm is able to bend in several directions, and it is controlled by *ad hoc* algorithms and software [7]. In [8] the authors study the feasibility and the design of a robotic octopus arm, starting with a study on the arm muscles and finishing with bending experiments on a cylindrical mock–up. In [9] the Active Hose is presented, that consists of curved units with a prismatic unit in their middle, and that is driven by pneumatic energy.

To our knowledge, the first attempt to integrate, in the same soft robot, locomotion and grasping capability has been presented in [10]. In [10] a platform with one soft limb has been developed, taking as a reference the biological observation on the octopus crawling behaviour. This platform is able to locomote and to wrap around objects. In this robot, stability was provided by two wheels and a third contact point, while the limb only provided for the motion. Despite this robot shows the feasibility of this dual–purpose of the limb, the robot presented is impractical for real application.

The robot developed hereafter has soft limbs, it uses a novel mechanism–specific gait in locomotion and it uses a cable actuation to wrap around objects. The robot is inspired, but not mimed, from *Octopus vulgaris*, and it was tested in water. In section II the biological background and analysis are summarized. In sections III–IV the robot design and development are presented, with the main features copied from the biological to the robotic field. In section V the experimentations carried out with the platform are introduced and the results are reported. Section VI concludes the paper summarizing the achievements.

II. BIOLOGICAL BACKGROUND

Crawling is a typical way of locomotion of octopuses on the seabed or along rocks in shallow waters or outside of the water. In an ongoing study on the kinematic properties of the octopus arms during crawling, mature octopuses were videotaped from underneath while crawling and sections of interest of the video clips were stored as single images. The position and state (attached to the substrate or not) of groups of suckers that were involved in the behaviour and the location of the mouth were labelled on consecutive images for further analysis (Fig. 1). Calculating the velocity and direction of movement of the labelled points and the distances between the suckers and between the suckers and the mouth, it was concluded that (1) during crawling, the octopus uses its arms only for pushing by elongation, (2) the direction of crawling is determined at each point in time by the direction of a simple vectorial combination of 1 to 4 arms employed in the task, (3) the crawling direction is changed by choosing a suitable set of arms to use for

M. Calisti, A. Arienti, F. Renda, P. Dario and C. Laschi are with The BioRobotics Institute, Scuola Superiore Sant'Anna, Pisa, Italy marcello.calisti@sssup.it

B. Hochner and G. Levy are with the Hebrew University of Jerusalem, Jerusalem, Israel

B. Mazzolai, is with The Centre for Micro-BioRobotics@SSSA, Istituto Italiano di Tecnologia (IIT), Pontedera (Pisa), Italy

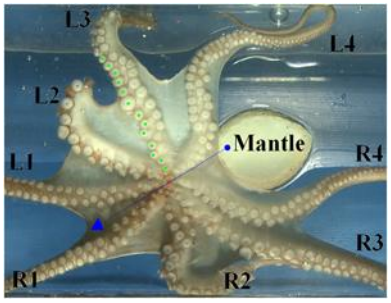

Fig. 1. An example of one labelled video image extracted out of a video clip in which an octopus was video taped from underneath while crawling. The arms are labelled according to their order from front to back, and side of the body (Left or Right). In this example the suckers of arm L3 are labelled (green dots), the mouth, which was considered as the centre of the animal, is labelled (red dot) and the direction of the animal's body (blue arrow), is defined to be the direction of the line running between the left and right arms and connecting the mid-point between the two most proximal suckers of each pair of L and R arms.

pushing rather than by rotating the body and (4) each of the participating arms demonstrate a stereotypical rhythmical behaviour composed of four repeated stages for pushing: (a) shortening the proximal segment of the arm (the part close to the centre of the body), (b) attaching a group of anchoring suckers to the substrate, (c) elongating the proximal segment of the arm to push the body, (d) releasing the anchoring suckers and again shortening the proximal segment for the beginning of the next step.

III. DESIGN

To mimic the key features of the octopus pushing-based locomotion, highlighted in section II, a soft limb with shortening/elongating capabilities has been designed, together with a specific activation mechanism. The limb is composed by a proximal part which is made of a steel cable, connected to a distal part that consists of a silicone cone (Fig. 2b). This limb, that aims to emulate the function of the octopus arm during pushing, does not change stiffness as, in fact, does the octopus. The limb has a stiff part and a compliant part, and it pushes the robot forward by elongating the stiff part. The dimensions of the silicone cone were chosen to match the actual proportions of an octopus arm. The limb is attached to a base (Fig. 2a) and the activation mechanism moves the arm to replicate the sequence of steps illustrated in section II. Two bars linked with a rotational joint were used. The first one, called crank, is moved by a DC motor. The second bar is constrained by a roto–translational constrain. The mechanism is illustrated in Fig. 3 and the resulting loop of the distal part of the arm is shown in Fig. 4. While the mechanism is far from a biological copy, the functionality is quite well reproduced.

In order to perform the bending, one nylon cable has been embedded along one side of the limb. With this approach, the sequence of longitudinal muscles of the octopus arm is approximated with a tendon–like actuation. Specifically, the position of the actuation is mimed, while the way this actuation is realized is not. It is not possible to obtain a local bending, as sometimes the octopus does, but a global bending is obtained using just one cable. The coupling between the specific actuation and the conic shape of the silicone limb allows to arrange the limb in a spiral–like geometry, that is used to wrap around objects and perform a sort of grasping. The direction of the bend depends on the nylon cable positioning: if it is embedded on the left side of the limb, that is between the central axis of the cone and left side of the limb, the cable bends towards the left side of the limb. Similarly if the cable is embedded on the right, upper or lower side of the limb, it will bend the limb right, up or down. The effect of the gravity is neglected because the limb has density similar to the density of fresh water. In the present work, the cable is embedded to perform a bend in a plane parallel to the ground, and was not used during crawling.

Despite the limbs have both pushing and bending capabilities, to provide the locomotion they should be radially lodged on a central base, as occurs in the octopus. The radial distribution allows, with simple pushes, to move in every direction simply by changing the arms devoted to push. All the limbs of the robot, and the arms of an octopus, have the same capabilities (except in reproduction). The robot presented here can work even with four limbs, but to replicate the redundancy of the biological counterpart, six limbs have been implemented. This kind of redundancy is common in biological systems, and should be taken into account when designing bioinspired robots [11]. This redundancy allows the robot to hold an object while moving, or even to lose a limb and still locomote. A crucial element in a redundant system is the control strategy applied; the robot proposed here uses a control strategy based on a mechanism–specific gait that is invariant to the number of limbs of the robot. Finally, the octopus has a density similar to the density of sea water. This important feature allows the octopus to move with really low forces. The same ratio between the octopus arm and sea water has been obtained between the robot and fresh water.

IV. DEVELOPMENT

A. Soft limb

The commercial ECOFLEX™ silicone 00-30 was used to build the limbs. The nylon cable runs along the whole limb, approximately parallel and 1 mm inside the surface of the limb. The very end of the cable is fixed to a plastic element. The steel cable runs approximately axially for 20 mm along the proximal part of the limb and it is fixed with a plastic element. The total length of the steel cable is about 100 mm so that the total length of the arm is about 280 mm. Each limb has its own base: a rectangular polyvinyl chloride (PVC) element where two commercial DC motors are lodged. One motor is a MM10 type, coupled with a Worm Gear Box H.E. from Tamiya©. This motor actuates the steel cable providing the thrust for the pushing–based locomotion. One hole in the base provides the constrain for the steel cable movement. The other motor is a GM12a Mini Metal Gear Motor. This small motor, that provides the pulling force on the nylon cable,

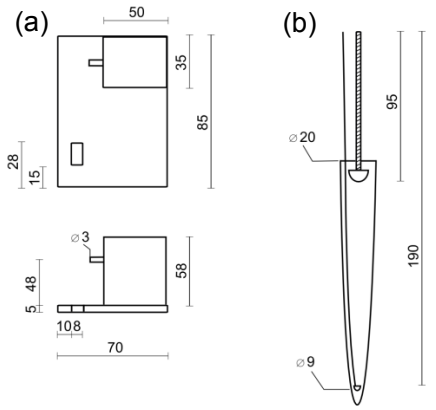

Fig. 2. In picture (a) the size (in mm) of the base is shown. The gearbox is represented as its containing volume. In picture (b) the internal structure of the soft limb, and its dimension, are shown.

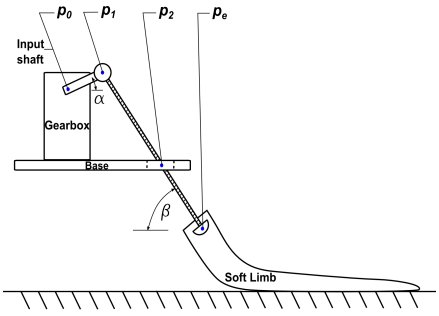

Fig. 3. The mechanical structure of a limb with its base, and the key points p_0, p_1, p_2 and p_e are shown. The motor that bends the limb is not shown.

is lodged over the gear box of the other motor, and bends the arm. A plastic crank, with a rotational link, transmits the rotational movement of the shaft of the gearbox to the steel cable. The actual dimensions of the limb and the PVC base are shown in Fig. 2.

The motion of the steel cable is a planar roto–translation, provided by the motors and constrained by the hole in the PVC base. The sketch of the structure, obtained from an orthogonal view of the plane of motion, is shown in Fig. 3. In this schematic depiction, $p_0 = (p_{0x}, p_{0y})$ is the coordinate of the centre of rotation of the crank, $p_1 = (p_{1x}, p_{1y})$ is the coordinate of the cylindrical link that connects the crank to the steel cable, $p_2 = (p_{2x}, p_{2y})$ is the coordinate of the hole, approximated to the centre, and $p_e = (p_{ex}, p_{ey})$ is the coordinate of the distal end of the steel cable, inside the silicone arm.

Referring to Fig. 3, the position of each point can be determined by geometrical calculation. Approximating, in free movement, the steel cable as a rigid body, and considering $l = 95$mm the length of the steel cable, and $m = 21$mm the length of the crank, the following (1)–(5) describe the positions of the structure as a function of α:

$$p_1 = (p_{0x} + m\cos\alpha, p_{0y} + m\sin\alpha) \tag{1}$$

$$p_e = (p_{2x} - b\cos\beta, p_{2y} - b\sin\beta) \tag{2}$$

$$l = \overline{p_1p_2} + \overline{p_2p_e} = a + b \tag{3}$$

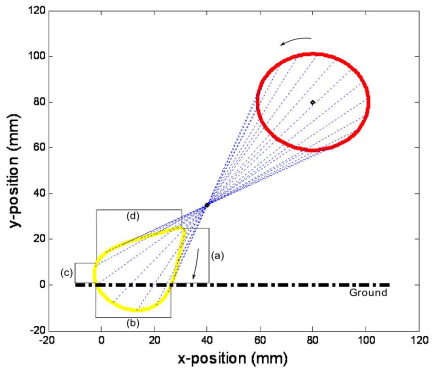

Fig. 4. The loop shape of the structure is presented. The circular shape in red, in the upper part of the picture, is the track of p_1. The shape in yellow, in the lower part of the picture, is the track of the point p_e. The black diamonds are p_0, above, and p_2, below. The blue dashed lines that connect the red track to the yellow one represent the steel cable. $y = 0$ is taken as the ground level.

$$b = l - \sqrt{(p_{1x} - p_{2x})^2 + (p_{1y} - p_{2y})^2} \tag{4}$$

$$\beta = \arctan\frac{p_{1y} - p_{2y}}{p_{1x} - p_{2x}} \tag{5}$$

From (1)–(5), with the coordinates $p_0 = (80, 80)$ and $p_2 = (40, 35)$, the resultant loop shape is shown in Fig. 4.

Considering an anticlockwise rotation of the input shaft, the loop in Fig. 4 reproduces the four steps introduced in section II: when p_e moves down without touching the ground, (a) in figure, it mimics the attaching phase, when p_e moves down and rear touching the ground (b), mimics the pushing phase, when p_e moves up (c), mimics the releasing phase and finally when p_e moves closer to the base (d), mimics the shortening phase, and the cycle can start over. This cycle is the fundamental kinematics of the pushing–based locomotion that is implemented in the six–limbs robot.

B. Bending mechanics

So far the structure of the limb that provides the pushing–based locomotion was described, but this limb can also perform bending. This bending is provided by a nylon cable: when the cable is pulled, it distributes a load to a side of the arm, producing a bend with increasing curvature from the base to the tip of the limb. In Fig. 5 the gross structure and the mechanics of this movement are shown.

The law of bending underlying the tendon–driven robot arm has been developed in [12]. The equations found there allow to obtain the deformations value (in a planar steady state condition) of the limb by knowing the geometric parameters and the tension of the cables immersed inside the body. The resulting equations of that work are reported below:

$$q = \frac{T(aRk - 1)}{E\pi R^2} \tag{6}$$

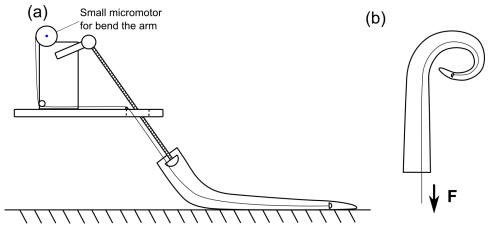

Fig. 5. In picture (a) the position of the small micromotor that pulls the cable is shown. The cable is embedded to the right side of the arm to provide the limb bending. The bending is shown in picture (b): the cable, when pulled, exerts a distributed load to a side of the arm, providing a bending with increasing curvature, from the base to the tip.

$$\frac{d}{ds}k = k(\frac{dR/dsR[-E\pi R^2 - T2a^2}{R^2[E(\pi/4R^2 + Ta^2} + \frac{TadR/ds}{R^2[E(\pi/4)R^2 + Ta^2} \quad (7)$$

$$k(l) = \frac{TaR(l)}{Ta^2R(l)^2 + E(\pi/4R(l)^4} \quad (8)$$

where k is the curvature of the robot arm and q the longitudinal strain (the Euler–Bernoulli beam hypothesis has been adopted) expressed in terms of the curvilinear variable $s \in [0, l]$. The radius of the section is R, and a is a scalar value that indicates the position of the cable with respect to the section (the distance from the tendon to midline is aR), E is the young modulus and T is the tension of the cable. The (6)–(8) have been changed to fit the soft limb described in this paper. As shown in Fig. 2 the distance between the cable and the midline is not proportional to the radius of the section, therefore the correct equations to be used are the following:

$$q = \frac{ky_cT - T}{E\pi R^2} \quad (9)$$

$$\frac{d}{ds}k = -k\frac{E\pi R^3 dR/ds + 2y_c dy_c/dsT}{ER^4\pi/4 + y_c^2T} + \frac{dy_c/dsT}{ER^4\pi/4 + y_c^2T} \quad (10)$$

$$k(l) = \frac{bT}{b^2T + ER(l)^4\pi/4} \quad (11)$$

where y_c represents the correct distance between the cable and the midline and has the linear expression below where a is the distance at the tip level and b is the distance at the base level, $y_c = (\frac{b-a}{l})s + a$. Still in [12] it is shown how, thanks to the Frenet Serrat formulas, the midline position can be derived from the deformations value, as illustrated below:

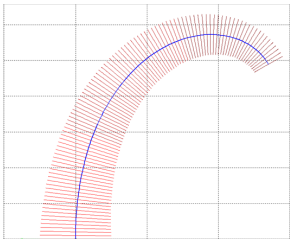

Fig. 6. Bending result for cable tension equal to 1N, $E = 110$kPa, $L = 100$mm, $R_{min} = 4.5$mm, $R_{max} = 10$mm, $b = 3.5$mm and $a = 9$mm.

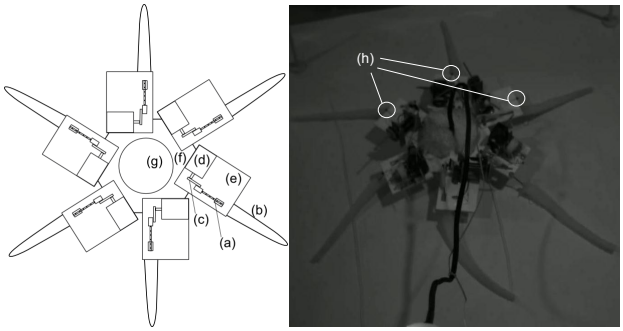

Fig. 7. The whole robot is composed by 6 steel cables (a), silicone limbs (b), cranks (c), gearboxes (d), 1 hexagonal central base (f) and one cylindrical float (g). 6 markers (h) were attached to the bases of the limbs; these markers were tracked with two cameras to obtain a 3–dimensional reconstruction of the robot during crawling.

$$\frac{d}{ds}(\overrightarrow{t}) = k(1+q)\overrightarrow{n}$$
$$\frac{d}{ds}(\overrightarrow{n}) = -k(1+q)\overrightarrow{t}$$
$$\frac{d}{ds}(\underline{u}) = (1+q)\overrightarrow{t}$$

where t and n represent the local reference frame and u the midline position vector. Fig. 6 shows the midline position described by (9)–(11) for a tension $T = 1$N.

C. Overall structure

The whole robot structure is presented in Fig. 7. The 6 limb bases are connected by a central hexagonal element, with a side $s = 80$mm. A float has been lodged over the central base to enforce the desired density ratio between salt water and octopus body. It is clear that in water a density similar to the density of the water helps to move with less forces: this characteristic seems to be essential to the octopus movements, and indeed it is replicated in the robot presented here. To obtain a floating condition, the following condition is required:

$$F_b = F_w$$
$$\rho_{water}gV = \rho_{robot}gV \quad (12)$$

Where F_b and F_w are respectively the buoyancy force and the weight force, g is the gravitational acceleration, V

TABLE I

THE MASS, VOLUME AND DENSITY OF EACH COMPONENT.

Component	Mass (g)	Volume (cm^3)	Density (g/cm^3)
Steel cable	1.81	0.30	6.07
Silicone limb	34.03	31.80	1.07
Limb base	17.60	29.23	0.60
Motor	16.81	7.59	2.22
Hexagonal base	50.05	83.14	0.60

the volume of fluid displaced, ρ_{water} the water density and ρ_{robot} the average value of density of the robot. This value has been obtained as the ratio between the mass of the robot and the total volume of the robot itself. The characteristics of the various parts of the robot are reported in table I.

For the octopus the buoyancy ratio is $\rho_{Swater}/\rho_{octopus} = 0.985$, with density of sea water $\rho_{Swater} = 1.025 g/cm^3$ and density of the octopus arm $\rho_{octopus} = 1.040 g/cm^3$ [13]. To achieve a similar ratio, a cylindrical float of radius $r = 45\ mm$ and height $h = 20$mm has been lodged on the robot, for a $V_{float} \simeq 127 cm^3$, that leads to a $\rho_{Fwater}/\rho_{robot} = 0.979$ and to a resulting vertical force of $F_y = F_b - F_w \simeq -0.16$N.

D. Crawling mechanics

The limbs and their activation strategy, introduced in subsection IV-A, allow a pushing–based locomotion. On a planar ground, this movement is effective if the height of the robot, in respect to the ground, is properly controlled. Referring to the loop of p_e in Fig. 4, it is clear that the robot could stand at a certain height between the lowest part and the highest part of the loop. This stance is provided by 4 limbs, called *stabilizing limbs*, that place p_e at the same point of the loop, controlling the height of the robot. In the example presented, they are placed to hold the robot at a specific height above the ground, referred to p_0, of 80mm. The remaining 2 limbs, called *propulsive limbs*, provide the pushing action needed for locomotion. When they touch the ground, they start to lift and move forward the robot. While the rear limb moves in the anticlockwise rotation shown in Fig. 4, the frontal limb moves in a clockwise rotation, or *vice versa* to inverte locomotion direction, with the same laws mentioned before. This provides a gait that is a combination of a pushing and pulling action. This gait is strictly related to the limb mechanism; this mechanism provides a simple cycling movement, that in the overall robot allows an omnidirectional locomotion, and in this sense the crawling of the robot is called a mechanism-specific gait.

To perform the locomotion, an *ad hoc* manual controller has been built. It is composed by 6 switches that allow to drive the motors in both direction. The sequence of locomotion is composed by 4 phases: (i) the locomotion is initiated achieving a desired height with the stabilizing limbs; (ii) the frontal limb is moved until it contacts the ground and then (iii) the same procedure is done with the rear limb. When both the propulsive limbs touch the ground, (iv) the motors are driven simultaneously and the robot moves one step forward. The procedure can be iterated changing the propulsive limbs to change direction. To evaluate the movement for each step, the contact between p_e and the ground is considered as a high friction contact that sticks the limb to the ground. In this way the displacement for each step is evaluated as the length of the phase (b) of the loop in Fig. 4.

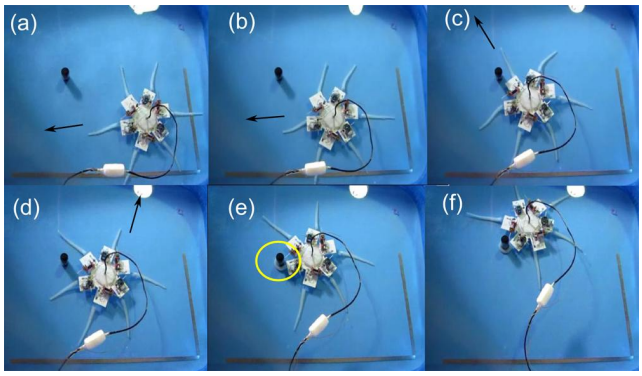

Fig. 8. From picture (a) to (f) 6 phases of a crawling and grasping action are shown. Selecting the appropriate pairs of limbs, it is possible to move in every direction, getting closer to the object. The arrows highlight the direction of the locomotion in each picture. In picture (e) the robot wraps around the target with its limb, and in picture (f) it moves away holding the object. These pictures are extracted from a video attached to the paper.

V. EXPERIMENTAL RESULTS

The robot has been tested in fresh water in a small swimming pool. The tests aim to show the effectiveness of the solution and the correspondences to the analysis proposed in section IV. The robot was recorded from above, with a camera placed over the swimming pool, and from one side with an underwater camera. A sequence of frames extracted from the recording is shown in Fig. 8.

It is shown that the robot is able to move in a desired direction by controlling just two limbs. As mentioned in section III, the redundancy in the system does not entail a complexity increase in the control. After the initial control of the height of the robot, that involves all the stabilizing limbs, the locomotion is performed by simply coordinating two limbs. Once the robot gets closer to the object, the second motor that pulls the nylon cable is activated to wrap around it. In this test, just one arm has been used to wrap around the object, but similarly the others could be employed. As explained in section III, the nylon cable bends the arm in the direction where the cable is placed. For this experiment, we embedded the nylon cable to obtain a bending approximately parallel to the plane of the ground. This is possible because the displacement due to the gravity, that is a distributed load on the limbs, is partially compensated by the buoyancy force. However, even if the bend is not planar, grasp could be still effective if the arm manages to wrap around the object, as shown in Fig. 8. Once the wrapping is complete, while one limb holds the object, the others push and pull the robot to move away.

During the experiments, a 3–dimensional tracking of the

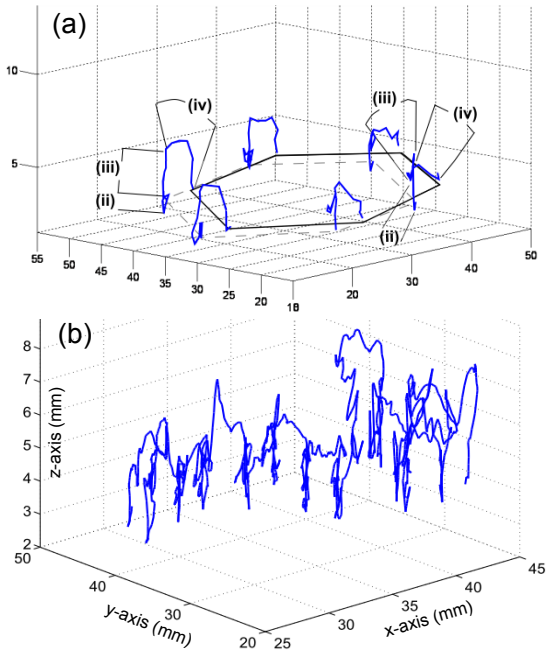

Fig. 9. In picture (a), the tracks of the markers of the bases, phases (ii)-(iv), during one step are shown. In picture (b) the track of the central point of the robot during several steps is shown.

markers shown in Fig. 9 was obtained. Two commercial cameras and an *ad hoc* software were used to retrieve markers positions into the 3–dimensional space. The performances of this kind of friction based locomotion have great variability, and also the coordination between frontal and rear limbs should be accurate to increase the effectiveness of the action. In order to evaluate the correspondence to the analysis presented in section IV-D, the track of the six bases is shown in Fig. 9a. The phase (i) of the locomotion procedure is not shown in the picture. During phase (ii), the robot touches the ground with the frontal limbs, lifting its frontal part. During phase (iii) the robot lifts its rear part, and finally during phase (iv) the movement is achieved driving both motors simultaneously. The track of the central point of the robot in Fig. 9b shows again the phases (i-iii) when the robot touches the ground with the limbs, and the phase (iv) when the robot moves its body to another position. The maximum displacement of the central point of the robot is about 26.4mm, while the displacement theoretically achievable of 28.1mm. Each step, from phase (i) to the end of phase (iv), was performed in an average value of 1.32 seconds, leading to a step speed of about 20mm/s. During this experimentation, the step frequency was intentionally low to focus the investigation on the stepping mechanism, and a delay was inserted between two consecutive steps. Increasing the step speed or decreasing the delay between steps will increase the crawling speed.

VI. CONCLUSIONS

In this paper a novel robotic system, with soft limbs able to push and to bend, has been illustrated. Taking as a reference biological studies on the octopus, a functional synthesis has been inferred to build a robot effective both in locomotion and grasping. The octopus has been adopted as inspiration in the limbs positioning and structure, in the water to body interaction and in the pushing–based locomotion strategy. The design, development and test of a six–limbs robot were analyzed. A mechanism-specific gait, that is simple and effective, was used: while several limbs provide the stability and a proper balancing, 2 or more limbs provide the effective pushing to move the robot forward. Electing different limbs, the direction is changed without increasing the complexity of the control strategy. The redundancy in the platform allows reliability from serious damages, from unexpected failures or loss of limbs, and it also allows to perform more tasks simultaneously, i.e. several wrappings around of different objects. The outcome from the present work can be regarded as a positive addition to the emerging field of soft robotics.

VII. ACKNOWLEDGEMENTS

This work was supported in part by the European Commission in the ICT-FET OCTOPUS Integrating Project, under contract no.231608

REFERENCES

[1] D. Trivedi, C. Rahn, W. Kier, and I. Walker, "Soft robotics: biological inspiration, state of the art, and future research," *Applied Bionics and Biomechanics*, vol. 5, pp. 99–117, 2008.

[2] M. A and D. P, "Bio-inspired solutions for locomotion in the gastrointestinal tract: background and perspectives," *Phil. Trans. R. Soc. A*, vol. 361, pp. 2287–2298, 2003.

[3] S. Seok, C. Onal, R. Wood, D. Rus, and S. Kim, "Peristaltic locomotion with antagonistic actuators in soft robotics," in *IEEE Int. Conf. on Robotics and Automation Conference Proceedings*. IEEE, May 2010.

[4] A. S. Boxerbaum, H. J. Chiel, and R. D. Quinn, "A new theory and methods for creating peristaltic motion in a robotic platform," in *IEEE Int. Conf. on Robotics and Automation Conference Proceedings*. IEEE, May 2010.

[5] Y. Sugiyama and S. Hirai, "Crawling and jumping of deformable soft robot," in *Proc. IEEE/RSJ Int. Conf. On Intelligent Robots and Systems*. IEEE/RSJ, September 2004, pp. 3276–3281.

[6] E. Steltz, A. Mozeika, N. Rodenberg, E. Brown, and H. Jaeger, "Jsel: jamming skin enabled locomotion," in *IEEE/RSJ Int. Conf. on Intelligent Robots and Systems*. IEEE/RSJ, October 2009, pp. 5672–5677.

[7] D. Trivedi, A. Lotfi, , and C. D. Rahn, "Geometrically exact models for soft robotic manipulators," *IEEE Transaction on robotics*, vol. 24, no. 4, August 2008.

[8] C. Laschi, B. Mazzolai, M. Cianchetti, and P. Dario, "Design of a biomimetic robotic octopus arm," *Bioinsp. Biomim.*, vol. 4, 2009.

[9] H. Tsukagoshi, A. Kitagawa, and M. Segawa, "Active hose: an artificial elephant's nose with maneuverability for rescue operation," in *Proc. IEEE Int. Conf. Robotics and Automation*. IEEE, 2001, pp. 2454–2459.

[10] M. Calisti, M. Giorelli, G. Levy, B. Mazzolai, B. Hochner, C. Laschi, and P. Dario, "An octopus-bioinspired solution to movement and manipulation for soft robots," *Bioinsp. Biomim.*, vol. 6, 2011.

[11] R. Pfeifer, F. Iida, and J. Bongard, "New robotics: design principles for intelligent systems," *Artif. Life*, vol. 11, pp. 99–120, 2005.

[12] F. Renda, M. Cianchetti, M. Giorelli, B. Mazzolai, P. Dario, and C. Lasch, "Planar steady-state physical model for a cable-driven octopus-like arm manipulator," in *International workshop on bio-inspired robot*, April 2011.

[13] M. Calisti, A. Arienti, M. Giannaccini, M. Follador, M. Giorelli, M. Cianchetti, B. Mazzolai, C. Laschi, and P. Dario, "Study and fabrication of bioinspired octopus arm mockups tested on a multipurpose platform," in *IEEE/RAS-EMBS Int. Conf. on Biomedical Robotics and Biomechatronics*. IEEE/RAS-EMBS, September 2010.